ACS Macro Letters

Letter

pubs.acs.org/macroletters

Phase Behavior of Tapered Diblock Copolymers from Self-Consistent Field Theory

Jonathan R. Brown,[†] Scott W. Sides,[‡] and Lisa M. Hall*,[†]

[†]William G. Lowrie Department of Chemical and Biomolecular Engineering, The Ohio State University, 140 W 19th Avenue, Columbus, Ohio 43210, United States

[‡]National Renewable Energy Laboratory (NREL), 15013 Denver West Parkway, Golden, Colorado 80401, United States

Supporting Information

ABSTRACT: Tapered diblock copolymers are similar to AB diblock copolymers, but the sharp junction between the A and B blocks is replaced with a gradient region in which composition varies from mostly A to mostly B along its length. The A side of the taper can be attached to the A block (normal) or the B block (inverse). We demonstrate how taper length and direction affect the phase diagrams and density profiles using self-consistent field theory. Adding tapers shifts the order−disorder transition to lower temperature versus the diblock, and this effect is larger for longer tapers and for inverse tapers. However, tapered systems' phase diagrams and interfacial profiles do not simply match those of diblocks at a shifted effective temperature. For instance, we find that normal tapering widens the bicontinuous gyroid region of the phase diagram, while inverse tapering narrows this region, apparently due to differences in polymer organization at the interfaces.

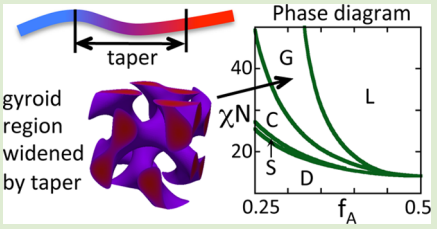

Amphiphilic molecules such as diblock copolymers, composed of two components that would tend to phase separate but are bonded into the same molecule, are well-known to microscopically phase separate to form various ordered structures.[1,2] For an AB diblock copolymer, the tendency to phase separate depends on the fraction of A monomers, f_A, and χN, where N is polymer length and the Flory χ parameter quantifies the degree to which A and B monomers tend to phase separate. A significant understanding of the microphase-separated morphologies as a function of polymer type and architecture has resulted from decades of experimental and theoretical work in this area, and many strategies to control the morphology by adjusting polymer type and architecture, adding homopolymers, or blending different copolymers together have been studied.[3,4] The ability to form bicontinuous phases is of special interest; for instance, in a polymer membrane used for separations or transport, one continuous phase could impart favorable mechanical properties while the other phase conducts ions.[5] Typical diblock copolymers can form bicontinuous phases, but the region of phase space where these are preferred is small, especially at high χN.[6] However, high molecular weight (large N) might be desired for mechanical properties. The fact that χN controls the phase behavior, but large N is required and χ depends on polymer choice (constrained by application-specific requirements), presents a fundamental restriction in design of these materials.

Linear tapered diblock copolymers, in which a linear gradient "block" is added between the pure A and B blocks of an AB diblock system (see Figure 1a), have attracted significant recent interest as a potential solution to this issue. The fraction of taper acts as an additional control parameter, and the taper can be in the normal or inverse direction as shown in Figure 1b. However, rational control of the microphase-separated state through tapering cannot be fully realized without a clear picture of how tapering adjusts the phase diagram. Predicting the theoretical phase diagram of model tapered copolymers is the major goal of the current work.

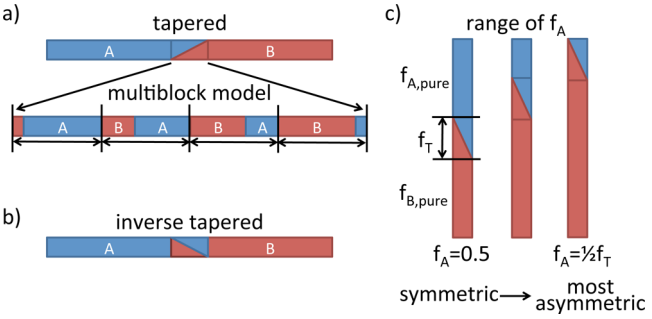

Figure 1. Schematic of the model. (a) A normal tapered copolymer: the A and B blocks are separated by a linear gradient "block", and the multiblock model is used to approximate the gradient region. The gradient region is made of multiple diblock domains of equal size; the fraction of A in each is varied along the region. (b) An inverse tapered polymer; the gradient region is reversed. (c) Examples showing the fraction of A (f_A) and fraction of taper (f_T); the taper can be placed in the middle of the polymer (left) or at the end of the polymer (right), or anywhere between these extremes.

Received: October 25, 2013
Accepted: December 3, 2013
Published: December 6, 2013

   dx.doi.org/10.1021/mz400546h | ACS Macro Lett. 2013, 2, 1105−1109

Experimental creation of diblock copolymer analogs but with a tapered or random AB midblock, or related adjustments to the sequence, has been possible for some time.[7−16] Several groups investigated how such changes affect the copolymers' microphase separation.[12−16] Recent experimental advances enabled creation of a set of well-controlled tapered diblock copolymers with various taper lengths and with both normal and inverse tapers.[5,17,18] These systems have also been well characterized; importantly, the bicontinuous gyroid phase was confirmed to exist for some volume fractions.[17] This partly motivates the current work, and some of the data such as the order−disorder transition (ODT) temperatures are useful as an initial check on the validity of the model.[18]

A large body of prior theory and simulation work determined the phase diagrams and density profiles of typical diblock copolymers and further considered triblocks and many other copolymer architectures.[3] In particular, linear gradient copolymers (100% length tapers) have been studied; for these only lamellar and disordered phases are predicted.[19,20] There has been relatively less attention paid to systems with modified interfaces such as tapers; one simulation study did consider various copolymer composition profiles incluiding a nonlinear gradient profile akin to our tapered profile.[21] Triblocks with a midblock of a random mixture of the end block monomers were also studied.[22,23] One may expect such a random midblock system's behavior to be between that of normal and inverse tapered systems, but it is unknown to what extent and how the details of the composition of the midblock affect microphase separation.

The consensus from prior theoretical diblock work is that the microphase-separated morphology is dictated by three effects: (1) the unfavorable interaction between A and B drives the interfacial area to be minimized with the restriction that the resultant morphology must fill space (the interface forms a minimal surface separating the two phases), (2) if the polymer is asymmetric, the interface tends to curve so the majority phase has more room to coil at the expense of stretching the minority phase, and (3) "packing frustration", meaning it is unfavorable for some chains to stretch much more than others (for some geometries this is required due to nonconstant curvature or to fill space given the placement of the interface). The lamellae structure has no curvature or packing frustration; cylinders have a high constant curvature and low packing frustration (due to stretching of some majority phase chains); and the gyroid has intermediate nonconstant curvature and high packing frustration.[3,24,25] Versus a typical diblock, we expect packing frustration is smaller for normal tapers: to fill space far from the interface, in addition to stretching a tapered polymer can slide out of place near the interface at a smaller free energy cost (the interface is more diffuse, and moving some of the taper into a lamella does not cost as much free energy as it would for a diblock). This effect should make the gyroid region wider. The taper also makes complete segregation of A and B difficult, implying the ODT moves to higher χN. It has been suggested[19] that a broad interface also decreases the propensity of the interface to curve. In the case of tapers, curvature may also be disfavored as it implies half of the taper has less room to coil than the other half, even though the two sides of the taper are mirror images of each other so would generally prefer to coil the same way. This would shift the curved phases toward more asymmetric systems. For normal tapers, this should be a relatively small effect since much of the taper is miscible with the pure block to which it is attached. These issues are complicated for inverse tapers as they may fold back and forth across the interface at large χN. It is not obvious which effects dominate for various systems, so here we use theory to predict the microphase-separated morphology as a function of taper length/direction.

In experimental systems, polydispersity, the details of the sequence randomness, and differences (such as in monomer size or stiffness) in A and B blocks could affect the system in important ways; in some cases, other bicontinuous phases could be preferred over gyroid. None of these effects are considered here, though some have been studied by others.[20,26−29] Potentially relevant to the idea that tapering may reduce packing frustration leading to widening of the gyroid window are studies of polydisperse systems. In these systems, short and long chains can be arranged in different locations to reduce packing frustration. The region of nonlamellar phases does widen as polydispersity increases; however, comparison is difficult as the different length chains can phase separate, and a mixture of lamellae and cylinder phases is present instead of gyroid at high χN.[29−31]

We used self-consistent field theory (SCFT) with a multiblock model of the taper to obtain phase diagrams and density profiles, and we applied the random phase approximation (RPA) to find spinodal curves using both the multiblock model and an exactly linear taper, as described in the Methods. Figure 2 shows the critical point as a function of taper size for both the normal and inverse tapered cases from the RPA (both linear and multiblock model) and SCFT (multiblock model). Notice that despite the relatively coarse multiblock model for the taper there is little disagreement between the RPA critical points for the exactly linear and coarser models. The maximum error is 5%, which occurs for large inverse tapers. The SCFT results lie nearly on top of the RPA results, although there is a small (<1%) error due to the

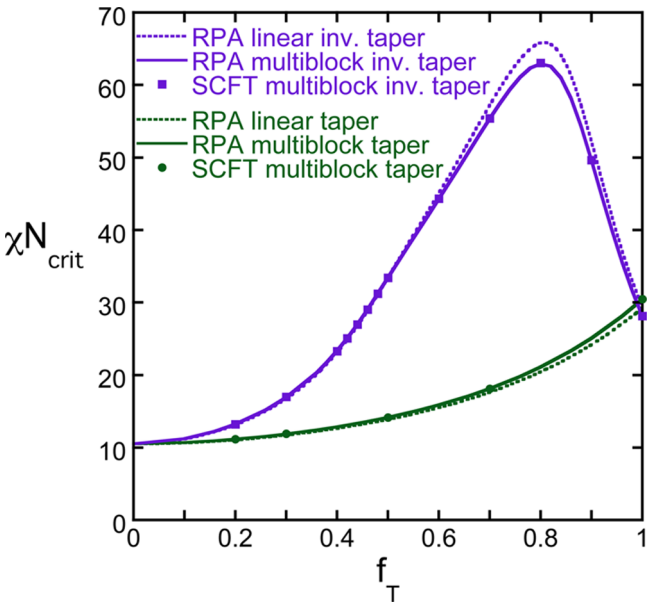

Figure 2. Critical point χN_{crit} for a symmetric system vs taper size (f_T) for normal (green) and inverse (purple) tapers. Solid curves are from the RPA with the multiblock model (see Figure 1a); dashed curves are for an ideal linear taper. Points are from SCFT with the multiblock model.

numerical difficulty of finding convergence of an ordered phase near the ODT using SCFT.

For normal tapers, as the taper gets wider, the increased difficulty of separating A and B means a larger χN is required to form ordered phases. The inverse tapered system shows such a trend at low f_T, but at a steeper rate, then its critical χN peaks and rejoins that of the normal taper at $f_T = 1$. For short tapers, the trend in $(\chi N)_{crit}$ is similar to that reported in experiment: for $f_T = 0.2$ the ODT of normal tapers is very similar to that of diblocks, but there is a much larger gap between the ODTs of the diblock and inverse tapered systems.[18] A polymer with a large inverse taper resembles an ABA′B′ tetrablock copolymer. However, for a large enough inverse taper, the pure blocks at either end of the taper are small and unimportant, so phase separation occurs more readily. Note that the inverse and normal tapered multiblock models are not exactly the same at $f_T = 1$. In a normal tapered system, the first and last blocks of the taper are very small (see Figure 1a), whereas in an inverse tapered system, the first and last blocks of the taper are the larger of the local AB pair. In the limit of $f_T = 1$, the pure blocks at either end are removed, so the terminal blocks of the taper become the terminal blocks of the polymer. It is therefore not surprising that the ODT for the inverse tapered system is slightly lower at $f_T = 1$. This difference along with the difference in the dashed and solid curves as a function of f_T give an idea of the accuracy of the multiblock model compared to an ideal gradient model. The coarse-grained nature of the multiblock model may actually better approximate certain experimental systems whose composition profile in the taper changes by small steps rather than truly linearly. This is due to a synthetic procedure during which the composition of the monomers is changed in a stepwise (rather than continuous) manner as the polymerization of the taper region proceeds.[17−19] However, neither model accounts for random variability of the gradient region, the details of which may be important in some cases; this has been explored for gradient copolymers but is not considered here.[20]

Extending beyond the symmetric case, Figure 3 shows the spinodal curves generated by the RPA for selected taper sizes as a function of f_A. For normal tapers, larger tapers shift the spinodal to larger χN, but the shape of the curve is largely unchanged. For a small inverse taper, the spinodal curve is similar to that of a normal taper shifted to even higher χN. Interestingly, for larger inverse tapers, the ordered phases become easier to form for the most asymmetric case than at slightly larger f_A. This is because for large inverse tapers there are significant nearly pure sections at either end of the taper, so a symmetric polymer acts like an ABA′B′ tetrablock, whereas the most asymmetric one acts like an ABA′ triblock.[35−37]

The major result of this study, phase diagrams for selected tapered systems, is shown in Figure 4. As expected, adding tapers shifts the ordered phases to higher χN, and this effect becomes even larger for more asymmetric polymers because many of the remaining minority (A) monomers are in the B side of the tapered portion and are unable to cleanly phase separate. The effect of adding tapers is not accounted for simply by adjusting the effective χN relative to the diblock. As expected if normal tapers act to relieve packing frustration, the gyroid region of the phase diagram is widened by the introduction of small to moderately sized normal tapers (see Figure 4ac). The diblock gyroid phase has previously been calculated to occur over a range in f_A of 0.037 at its widest extent,[38] whereas for the tapered systems, at $f_T = 0.3$ this width is 0.049, and for $f_T = 0.5$

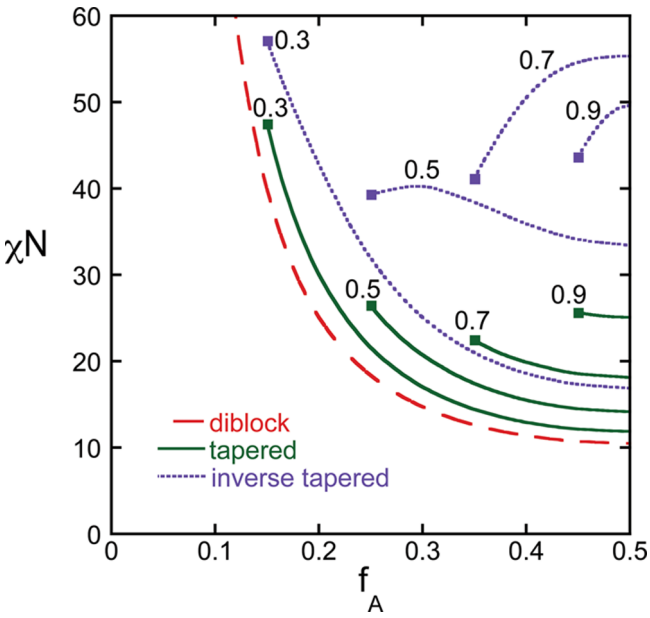

Figure 3. Spinodal curves as a function of total fraction of A (f_A) calculated using the RPA for diblock (red, dashed), normal tapered (green, solid), and inverse tapered (purple, dotted) copolymers, for four different taper sizes as labeled. The limit of the model occurs when the taper is at the end of the polymer. Therefore, the curves end at $f_A = (1/2)f_T$ (see Figure 1c), as indicated by the squares at the end of the curves. Note that, due to symmetry, considering $f_A > 0.5$ is unnecessary.

this width is 0.075 (also, for $f_T = 0.5$ and $\chi N > 49.3$, the only nonlamellar structure is gyroid). However, when $f_T = 0.7$, the region of nonlamellar ordered phases is very small because most of the polymer backbone is the taper, so there is only a small window of possible f_A values. Another effect to consider is that the increased interfacial width of these systems may reduce the tendency of the interface to curve. Since the interfacial width of the 30% normal tapered system is small (see Figure 5), the location of the curved phases is not noticeably shifted versus the diblock. However, at 50% normal taper, the curved phases are shifted slightly to smaller f_A, and the 30% inverse tapered case shows only a very small region of nonlamellar (higher curvature) ordered phases. This can also be seen by the location of the C/G/L triple point at $f_A = 0.450$, 0.444, and 0.419 for normal tapers with $f_T = 0.3$, 0.5, and 0.7, respectively (and at $f_A = 0.421$ for the 30% inverse tapers).

Lamellar density profiles corresponding to symmetric $\chi N = 80$ systems are shown in Figure 5 for the same four systems as in Figure 4. These density profiles are close to the limiting cases (they do not change much with further increases in χN). Intuitively, the wider taper creates a wider interface and lowers the maximum purity of A (or B) found in the middle of the lamellae. 30% inverse tapers have an extremely wide interface because the inverse taper is not able to orient itself along the interface as easily.

Figure 6 shows the lamellar domain spacing for symmetric diblock and normal and inverse tapered systems as a function of χN. For normal tapers, as in diblocks, as χN increases, spacing increases; the polymers stretch out to better segregate and reduce interfacial area. For inverse tapered systems, there is a different effect: for a large enough inverse taper (or high enough χN), the polymer looks like an ABA′B′ tetrablock, and to more cleanly order into a lamellar structure, it needs to fold

dx.doi.org/10.1021/mz400546h | ACS Macro Lett. 2013, 2, 1105−1109

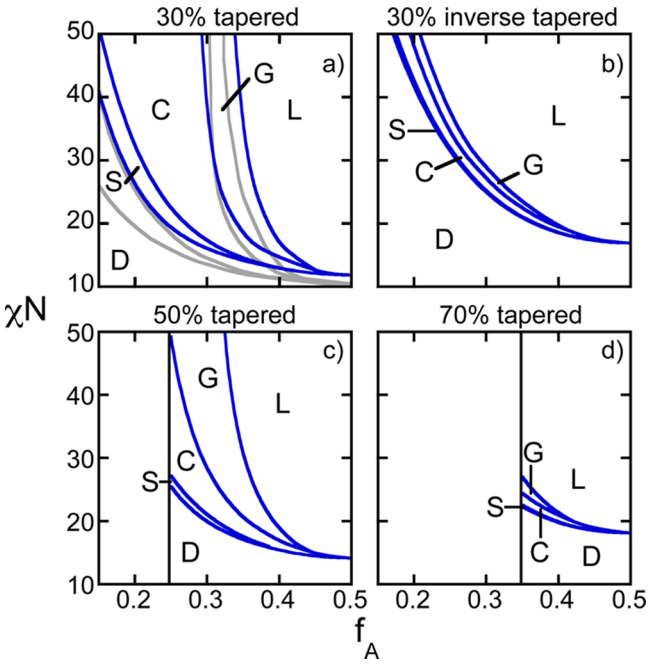

Figure 4. Tapered copolymer phase diagrams from SCFT (blue) for (a) 30% normal, (b) 30% inverse, (c) 50% normal, and (d) 70% normal tapers. Morphologies are labeled L for lamellae, G for gyroid, C for hexagonally packed cylinders, S for BCC spheres, and D for disordered (other phases were not considered). For comparison, the diblock SCFT phase diagram is shown in gray in part (a) (adapted from Cochran et al.[39]). The axis ranges of each plot are the same. The limit of the model occurs at $f_A = (1/2)f_T$ (see Figure 1c), so the 50% and 70% phase diagrams are limited to the right of the vertical lines at $f_A = 0.25$ and 0.35, respectively. The curves are approximate smoothed connections between the calculated phase boundary points (see the Supporting Information for the tabulated values).

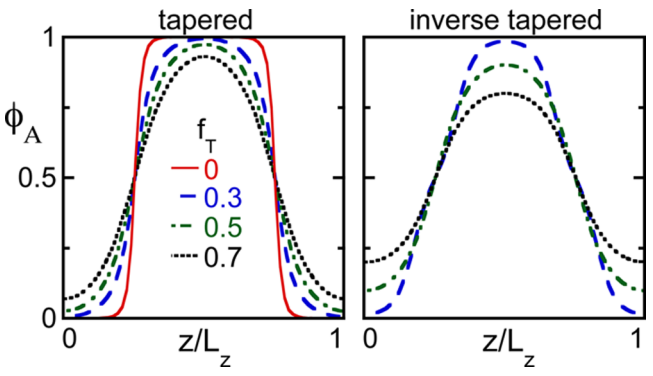

Figure 5. Lamellar density profile showing the volume fraction of A monomers (ϕ_A) versus perpendicular distance across the lamellae of width L_z at $\chi N = 80$ for symmetric ($f_A = f_B = 0.5$) systems for normal (left) and inverse (right) tapers. The red curve shows the diblock profile for comparison. The taper fractions are: $f_T = 0.3$ (blue, dashed), $f_T = 0.5$ (green, dash-dotted), and $f_T = 0.7$ (black, dotted).

back and forth across the interface or bridge between more than one lamellae.[37] Related folding or looping behavior was suggested to occur for experimental inverse tapered systems in solvent, based on the size of their micelles.[9] The inverse taper folding results in significantly smaller lamellae and depends on taper length and χN. The lamellar width of short inverse tapers is similar to that of normal tapers at low χN and initially increases as a function of χN, but due to increasing folding,

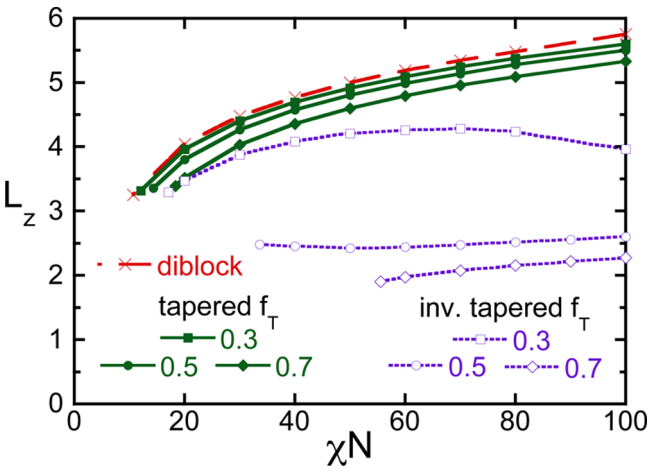

Figure 6. Lamellar spacing L_z vs χN for symmetric ($f_A = f_B = 0.5$) diblock (red, dashed line with exes), normal tapered (green, solid lines with filled symbols), and inverse tapered (purple, dotted lines with open symbols) systems with $f_T = 0.3$ (squares), $f_T = 0.5$ (circles), and $f_T = 0.7$ (diamonds).

lamellar width later decreases at larger χN. In contrast, large inverse tapered systems showed folding even near the ODT, so an increase in χN only slightly stretched them out.

We employed SCFT to determine the phase behavior of modified diblock copolymers that include a linear gradient region (taper) between the two blocks. The size of the taper can be used to control the phase behavior. As expected intuitively and from experimental work, the ODT of the tapered polymers moves to lower temperature or higher χN compared to pure diblocks. However, tapered systems are not the same as diblocks at a new effective χN; the morphology for a given composition may change as a function of taper size (and direction), and the density profiles can change significantly as well. Inverse tapers at high enough χN tend to fold back and forth across the interface, changing the lamellar spacing significantly versus the diblock. The result for certain inverse systems is a relative lack of change in the lamellar spacing as a function of χN, meaning inverse tapered systems may be attractive for applications where a constant spacing as a function of temperature is desired. Normal tapers are predicted to allow easier access to bicontinuous phases (only gyroid was considered here), especially relevant for transport or separations applications.

METHODS

The phase behavior of the tapered gradient copolymers was determined from SCFT as implemented in PolySwift++. The standard SCFT method employed assumes incompressible Gaussian (random walk) chains in a mean field that is generated self-consistently with the density field. Specifics of the model and the numerical solution method can be found in the Supporting Information and refs 32−34.

We also used the well-known RPA, which leads to relatively simple equations for the structure factor of copolymers in the disordered state, to compute the spinodal curves of the model system under the same assumptions employed in our SCFT calculations. For this we employ eqs 5 and 6 in Jiang et al.;[19] this is a simple integral calculation that finds the divergence of the first peak in the structure factor (where spinodal decomposition will occur) based on the composition profile of the polymer.

We use a "multiblock model" similar to the one of Jiang et al.[19] to approximate the gradient region in a way that is straightforward to implement in SCFT. In this model, the taper is made of alternating A

and B blocks; each AB pair is the same size, but the composition varies to approximate the gradient (see Figure 1). Each two-block division was 2% of the polymer length (e.g., a 30% taper would be made of 30 blocks), chosen to keep the computations reasonable while still having an accurate description of a linear gradient (see Figure 2).

Only the major diblock morphologies were considered: lamellae (L), double gyroid (G), hexagonally packed cylinders (C), and body-centered cubic (BCC) packed spheres (S). The minor phases (close packed spheres and the orthorhombic *Fddd* interpenetrating network) that occur on the full AB diblock SCFT phase diagram were not considered because: (1) they represent a very small portion of the phase diagram, (2) they do not change the overall picture (packing of spheres and differences between network phases are not of primary importance), and (3) including them significantly increases the computational requirements.[6]

■ ASSOCIATED CONTENT

Ⓢ Supporting Information

Numerical phase boundaries, details of the SCFT calculation, SCFT parameters and methodology, and interfacial spacing and width are shown. This material is available free of charge via the Internet at http://pubs.acs.org.

■ AUTHOR INFORMATION

Corresponding Author

*E-mail: hall.1004@osu.edu.

Notes

The authors declare no competing financial interest.

■ ACKNOWLEDGMENTS

LMH and JRB acknowledge partial support of this work from the H.C. “Slip” Slider Professorship in Chemical and Biomolecular Engineering. We also thank Thomas Epps, III for many helpful comments and suggestions over the course of this work.

■ REFERENCES

(1) Bates, F. S.; Fredrickson, G. H. *Phys. Today* **1999**, *52*, 32.
(2) Hamley, I. W. *The Physics of Block Copolymers*; Oxford University Press, Incorporated: New York, 1998.
(3) Matsen, M. W. *J. Phys.: Condens. Matter* **2002**, *14*, R21−R47.
(4) Mai, Y.; Eisenberg, A. *Chem. Soc. Rev.* **2012**, *41*, 5969−5985.
(5) Mastroianni, S. E.; Epps, T. H. *Langmuir* **2013**, *29*, 3864−3878.
(6) Tyler, C. A.; Morse, D. C. *Phys. Rev. Lett.* **2005**, *94*, 208302.
(7) Diamanti, S. J.; Khanna, V.; Hotta, A.; Coffin, R. C.; Yamakawa, D.; Kramer, E. J.; Fredrickson, G. H.; Bazan, G. C. *Macromolecules* **2006**, *39*, 3270−3274.
(8) Bühler, F.; Gronski, W. *Die Makromol. Chem.* **1986**, *187*, 2019−2037.
(9) Hodrokoukes, P.; Pispas, S.; Hadjichristidis, N. *Macromolecules* **2002**, *35*, 834−840.
(10) Samseth, J.; Spontak, R. J.; Smith, S. D.; Ashraf, A.; Mortensen, K. *J. Phys. IV* **1993**, *03*, C8-59−C8-62.
(11) Schmitz, C.; Mourran, A.; Keul, H.; Möller, M. *Macromol. Chem. Phys.* **2008**, *209*, 1859−1871.
(12) Hashimoto, T.; Tsukahara, Y.; Kawai, H. *Polym. J.* **1983**, *15*, 699−711.
(13) Laurer, J. H.; Smith, S. D.; Samseth, J.; Mortensen, K.; Spontak, R. J. *Macromolecules* **1998**, *31*, 4975−4985.
(14) Hasegawa, H.; Hashimoto, T.; Hyde, S. T. *Polymer* **1996**, *37*, 3825−3833.
(15) Tsukahara, Y.; Nakamura, N.; Hashimoto, T.; Kawai, H.; Nagaya, T.; Sugimura, Y.; Tsuge, S. *Polym. J.* **1980**, *12*, 455−466.
(16) Hodrokoukes, P.; Floudas, G.; Pispas, S.; Hadjichristidis, N. *Macromolecules* **2001**, *34*, 650−657.
(17) Roy, R.; Park, J. K.; Young, W.-S.; Mastroianni, S. E.; Tureau, M. S.; Epps, T. H. *Macromolecules* **2011**, *44*, 3910−3915.
(18) Singh, N.; Tureau, M. S.; Epps, T. H. *Soft Matter* **2009**, *5*, 4757−4762.
(19) Jiang, R.; Jin, Q.; Li, B.; Ding, D.; Wickham, R. A.; Shi, A.-C. *Macromolecules* **2008**, *41*, 5457−5465.
(20) Ganesan, V.; Kumar, N. A.; Pryamitsyn, V. *Macromolecules* **2012**, *45*, 6281−6297.
(21) Pakula, T.; Matyjaszewski, K. *Macromol. Theory Simul.* **1996**, *5*, 987−1006.
(22) Zielinski, J. M.; Spontak, R. J. *Macromolecules* **1992**, *25*, 5957−5964.
(23) Spontak, R. J.; Williams, M. C. *J. Macromol. Sci., Part B* **1989**, *28*, 1−24.
(24) Matsen, M. W.; Bates, F. S. *Macromolecules* **1996**, *29*, 7641−7644.
(25) Matsen, M. W.; Bates, F. S. *J. Chem. Phys.* **1997**, *106*, 2436.
(26) Matsen, M. W.; Schick, M. *Macromolecules* **1994**, *27*, 4014−4015.
(27) Tureau, M. S.; Epps, T. H. *Macromolecules* **2012**, *45*, 8347−8355.
(28) Matsushita, Y.; Noro, A.; Iinuma, M.; Suzuki, J.; Ohtani, H.; Takano, A. *Macromolecules* **2003**, *36*, 8074−8077.
(29) Widin, J. M.; Kim, M.; Schmitt, A. K.; Han, E.; Gopalan, P.; Mahanthappa, M. K. *Macromolecules* **2013**, *46*, 4472−4480.
(30) Matsen, M. W. *Phys. Rev. Lett.* **2007**, *99*, 148304.
(31) Sides, S. W.; Fredrickson, G. H. *J. Chem. Phys.* **2004**, *121*, 4974−4986.
(32) Sides, S. W.; Fredrickson, G. H. *Polymer* **2003**, *44*, 5859−5866.
(33) Drolet, F.; Fredrickson, G. H. *Phys. Rev. Lett.* **1999**, *83*, 4317−4320.
(34) Fredrickson, G. H.; Ganesan, V.; Drolet, F. *Macromolecules* **2002**, *35*, 16−39.
(35) Hamersky, M. W.; Smith, S. D.; Gozen, A. O.; Spontak, R. J. *Phys. Rev. Lett.* **2005**, *95*, 168306.
(36) Matsen, M. W. *J. Chem. Phys.* **2000**, *113*, 5539−5544.
(37) Since these large inverse tapered systems have significantly different behavior from the standard diblock, potentially leading to different microphase-separated states, further detailed discussion will be reserved for a future publication.
(38) Matsen, M. W.; Bates, F. S. *Macromolecules* **1996**, *29*, 1091−1098.
(39) Cochran, E. W.; Garcia-Cervera, C. J.; Fredrickson, G. H. *Macromolecules* **2006**, *39*, 2449−2451.